nature cell biology

Abi1 regulates the activity of N-WASP and WAVE in distinct actin-based processes

Metello Innocenti[1,2], Silke Gerboth[1,2], Klemens Rottner[3], Frank P. L. Lai[3], Maud Hertzog[1,2,5], Theresia E. B. Stradal[4], Emanuela Frittoli[1,2], Dominique Didry[5], Simona Polo[1,2], Andrea Disanza[1,2], Stefanie Benesch[3], Pier Paolo Di Fiore[1,2,6], Marie-France Carlier[5,7] and Giorgio Scita[1,2,7]

Neural Wiskott–Aldrich syndrome protein (N-WASP) and WAVE are members of a family of proteins that use the Arp2/3 complex to stimulate actin assembly in actin-based motile processes. By entering into distinct macromolecular complexes, they act as convergent nodes of different signalling pathways. The role of WAVE in generating lamellipodial protrusion during cell migration is well established. Conversely, the precise cellular functions of N-WASP have remained elusive. Here, we report that Abi1, an essential component of the WAVE protein complex, also has a critical role in regulating N-WASP-dependent function. Consistently, Abi1 binds to N-WASP with nanomolar affinity and, cooperating with Cdc42, potently induces N-WASP activity *in vitro*. Molecular genetic approaches demonstrate that Abi1 and WAVE, but not N-WASP, are essential for Rac-dependent membrane protrusion and macropinocytosis. Conversely, Abi1 and N-WASP, but not WAVE, regulate actin-based vesicular transport, epidermal growth factor receptor (EGFR) endocytosis, and EGFR and transferrin receptor (TfR) cell-surface distribution. Thus, Abi1 is a dual regulator of WAVE and N-WASP activities in specific processes that are dependent on actin dynamics.

Dynamic assembly of actin filaments generates the forces that support motile behaviour, which is critical for a variety of cellular processes, including cell shape changes, cell migration and cytokinesis[1,2]. The actin cytoskeleton is also implicated in endocytosis and vesicular transport[3].

In vivo, actin is assembled at a steady state. New filaments are initiated at the membrane in a site-directed fashion, by autocatalytic filament branching[1,2]. This reaction is catalysed by the N-WASP– or WAVE–Arp2/3 complex machinery, whose activation is induced by the small G proteins Cdc42 and Rac, respectively[4]. The modalities through which these proteins are regulated reveal unexpected levels of complexity. For instance, N-WASP is locked in an auto-inhibited state. Binding of regulatory signalling proteins such as Cdc42, and phospholipids such as phosphatidylinositol-4,5-phosphate (PtdIns(4,5)P_2), cooperate to relieve this inhibition[4]. Conversely, binding of WIP (WASP interacting protein) or its related protein CR16, to N-WASP results in the formation of an inhibited WIP/CR16–N-WASP complex, which exerts a critical role in integrating signalling cascades, leading to actin polymerization[5]. Additionally, a number of SH3-containing proteins, such as Nck and Grb2, have been reported to bind and activate WASP/N-WASP, often acting synergistically with either Cdc42 or PtdIns(4,5)P_2 (ref. 3). Among these proteins, endophilin A, intersectin, syndapin/pacsin and more recently cortactin, have been previously characterized as endocytic proteins, consistent with the involvement of N-WASP in transport/internalization processes[3].

Unlike N-WASP, WAVEs are endowed with constitutive activity, but their regulation is achieved via the formation of macromolecular complexes[6]. The majority of both WAVE1 and -2 in cells is in a complex with: Nap1, an Nck-associated protein[7]; PIR121/Sra-1, identified as a Rac effector[8]; HSPC300, a small protein (with relative molecular mass 9,000; M_r 9K)[9]; and Abi1, an Abl-binding partner[10]. Whether WAVE is active or maintained inactive within this complex is still a matter for debate[9,11]. Whatever the case, Abi1 is an essential component of this complex, positively regulating WAVE activity *in vitro*, and connecting WAVE to Rac through the assembly of a WAVE–Abi1–Nap1–PIR121 complex[11–13].

Thus, a model is emerging whereby N-WASP/WAVE family members, by assembling into multi-molecular units, act as convergent nodes of different signalling inputs regulating actin dynamics in a variety of different processes. Functionally, however, whereas WAVEs have been demonstrated to be essential for Rac-dependent actin remodelling[11,14,15], the cellular role(s) of WASP/N-WASP has remained largely elusive.

Here, starting with the unexpected discovery that Abi1 — a key component of the WAVE complex — also binds and potently activates N-WASP, we utilized a combined biochemical, cell biological, and molecular genetic approach to define the modalities through which functional specification of WAVE and N-WASP activity, via Abi1, is achieved.

[1]IFOM, Istituto FIRC di Oncologia Molecolare, Via Adamello 16, 20134, Milan, Italy. [2]Department of Experimental Oncology, Istituto Europeo di Oncologia (IEO), Via Ripamonti 435, 20141, Milan, Italy. [3]Cytoskeleton Dynamics Group, [4]Signalling and Motility Group, German Research Centre for Biotechnology (GBF), Mascheroder Weg 1, D-38124 Braunschweig, Germany. [5]Dynamique du Cytosquelette Laboratoire d'Enzymologie et Biochimie Structurales, C.N.R.S. 91198 Gif-sur-Yvette, France. [6]Dipartimento di Medicina, Chirurgia ed Odontoiatria, Universita' degli Studi di Milano, 20122 Milan, Italy.
[7]Correspondence should be addressed to G.S. (e-mail: giorgio.scita@ifom-ieo-campus.it) or M.F.C. (e-mail: carlier@lebs.cnrs-gif.fr)

Received 17 June 2005; accepted 18 August 2005; published online: 11 September 2005; DOI: 10.1038/ncb1304

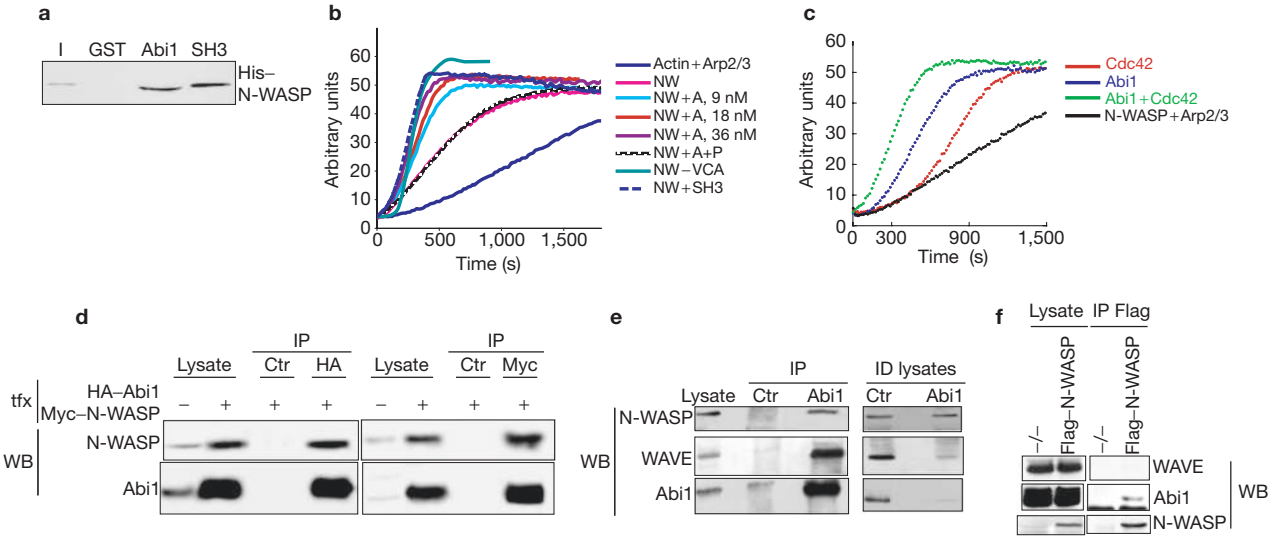

Figure 1 Abi1 binds to and activates N-WASP. (**a**) Abi1 binds directly to N-WASP. His-tagged N-WASP (1.25 μM) was incubated with 5 μM of immobilized GST–Abi1, or its SH3 domain, or GST. After washing, bound N-WASP was eluted, resolved by SDS–PAGE and detected with anti-His antibodies. The input (I) lane was loaded with 0.125 μM N-WASP. (Input corresponds to 10% of total). (**b**) Abi1 activates N-WASP and Arp2/3-dependent actin polymerization. Kinetics of Arp2/3-mediated polymerization of the VCA domain of N-WASP (30 nM; NW-VCA), or of full-length N-WASP (30 nM) in the absence (NW) or the presence of the indicated concentrations of Abi1 (NW + A) or the isolated SH3 domain of Abi1 (500 nM; NW+SH3), used at a saturating concentration. A 500 molar excess of a Sos-1-derived peptide dimer VPPPVPPRRR-Aha-K-Aha-RRRPPVPPPV (P)[20,21] was also used together with N-WASP and 18 nM of Abi1 (NW + A + P). (**c**) Abi1 synergizes with Cdc42 in activating N-WASP. Kinetics of Arp2/3 (50 nM)-mediated polymerization of N-WASP (20 nM) in the presence of saturating concentrations of Abi1 (230 nM), GTP-loaded Cdc42 (2,200 nM) or Abi1 and GTP-loaded Cdc42. (**d**) Abi1 and N-WASP associate *in vivo*. Lysates of 293T cells, coexpressing HA–Abi1 and Myc–N-WASP (tfx), were immunoprecipitated (IP) with control (ctr; anti-AU5), HA or Myc antibodies. Lysates (1/20 of the total) from mock (–) or Abi1- and N-WASP-transfected (+) cells and immunoprecipitates were immunoblotted with the indicated antibodies (WB). (**e**) Endogenous Abi1 and N-WASP co-immunoprecipitate. Total cellular lysates (2 mg) of growing HeLa cells were immunoprecipitated with anti-Myc, as a control (ctr), or anti-Abi1 antibodies. Lysate (50 μg), immunoprecipitates, and lysates after immunodepletion (ID lysates) with a control or with anti-Abi1 (Abi1) antibodies were resolved by SDS–PAGE and immunoblotted with the indicated antibodies. (**f**) Abi1, but not WAVE, co-immunoprecipitates with N-WASP. N-WASP-null fibroblasts[24] were stably transfected with empty (–/–) or Flag-tagged N-WASP (Flag–N-WASP) vectors. Total cellular lysates (10 mg) were then immunoprecipitated with anti-Flag antibody. Lysates, N-WASP-immunodepleted lysates (25 μg) (see Supplementary Information, Fig. S1b), and immunoprecipitates were immunoblotted (WB) with the indicated antibodies. The lower bands in the Abi1 immunoblot are IgG.

Abi1 is a scaffolding protein that permits the assembly of different multi-molecular complexes[6,16,17] including the WAVE–Abi1–NAP1–PIR121/Sra1 complex, which is essential for the formation of membrane protrusions where it specifically localizes[11,15]. Notably, the other major member of the WASP/WAVE family, N-WASP, has also been reported to exist in an activated state in lamellipodia[18]. Moreover, at least in *Drosophila*, the homologue of Abi1 binds WASP, predicting a role in N-WASP/WASP-dependent actin dynamics[19]. To explore this possibility, we tested whether Abi1 and N-WASP interact *in vitro* and *in vivo*.

Recombinantly produced and purified Abi1 and N-WASP formed a complex *in vitro*, indicating that their interaction is direct (Fig. 1a). Mapping of the interaction surfaces revealed that the SH3 domain of Abi1 mediates the binding to N-WASP (Fig. 1a). Actin polymerization assays showed that N-WASP was activated by Abi1 to stimulate actin polymerization (Fig. 1b). Abi1 was effective at concentrations in the nanomolar range, and exhibited a saturation behaviour. Maximum stimulation was observed at Abi1 concentrations similar to N-WASP (10^{-8} M), consistent with a M_r value in the nanomolar range for the Abi1–N-WASP complex (Fig. 1b and Supplementary Information, Fig. S1a). The activation of N-WASP by Abi1 was relieved by the Sos-1-derived peptide, which inhibits the activation of N-WASP by the SH3 domain of Grb2 (ref. 20), and the SH3-mediated interactions of Abi1 (ref. 21), indicating that the binding of the SH3 domain of Abi1 to N-WASP is required for activation. Accordingly, the isolated SH3 domain of Abi1 activated N-WASP (Fig. 1b and Supplementary Information, Fig. S1a) with a half-effect (the concentration at which half-maximal stimulation is seen) similar to that of the N-terminal SH3 domain of Grb2 (see Supplementary Information, Fig. S1a). Notably, the half-effect of full-length Abi1 was at a concentration 45-fold lower than that of the isolated SH3 domain (680 nM) (see Supplementary Information, Fig. S1a), suggesting that additional residues of Abi1 are needed for full activity. Direct comparison between Abi1 and Grb2 indicated that the concentration of full-length Abi1 leading to half-maximal stimulation of N-WASP (15 nM) was sevenfold lower than that of Grb2 (115 nM) (see Supplementary Information, Fig. S1a), supporting the notion that Abi is one of the most potent SH3-containing activators[22] of N-WASP. Notably, Abi1 is much more effective in N-WASP than in WAVE activation, for which a half-effect of about 0.2 μM was recorded[11]. Moreover, the activation of N-WASP by one molar equivalent of Abi1 was not affected by addition of Nap1–PIR121 complex (data not shown). Finally, Abi1 synergized with Cdc42 (Fig. 1c), but not with PtdIns(4,5)P_2 (data not shown), in activating N-WASP when both proteins were used at saturating concentrations. Because the binding affinity between Cdc42 and N-WASP (K_d = 0.45 μM) was not affected by Abi1 (data not shown), the cooperative effect on N-WASP-dependent actin polymerization reflects the ability of Cdc42 and Abi1 to simultaneously bind N-WASP at distinct sites in a ternary complex that shows maximal activity, supporting the view that Cdc42 and Abi1 regulate N-WASP in a coordinated fashion.

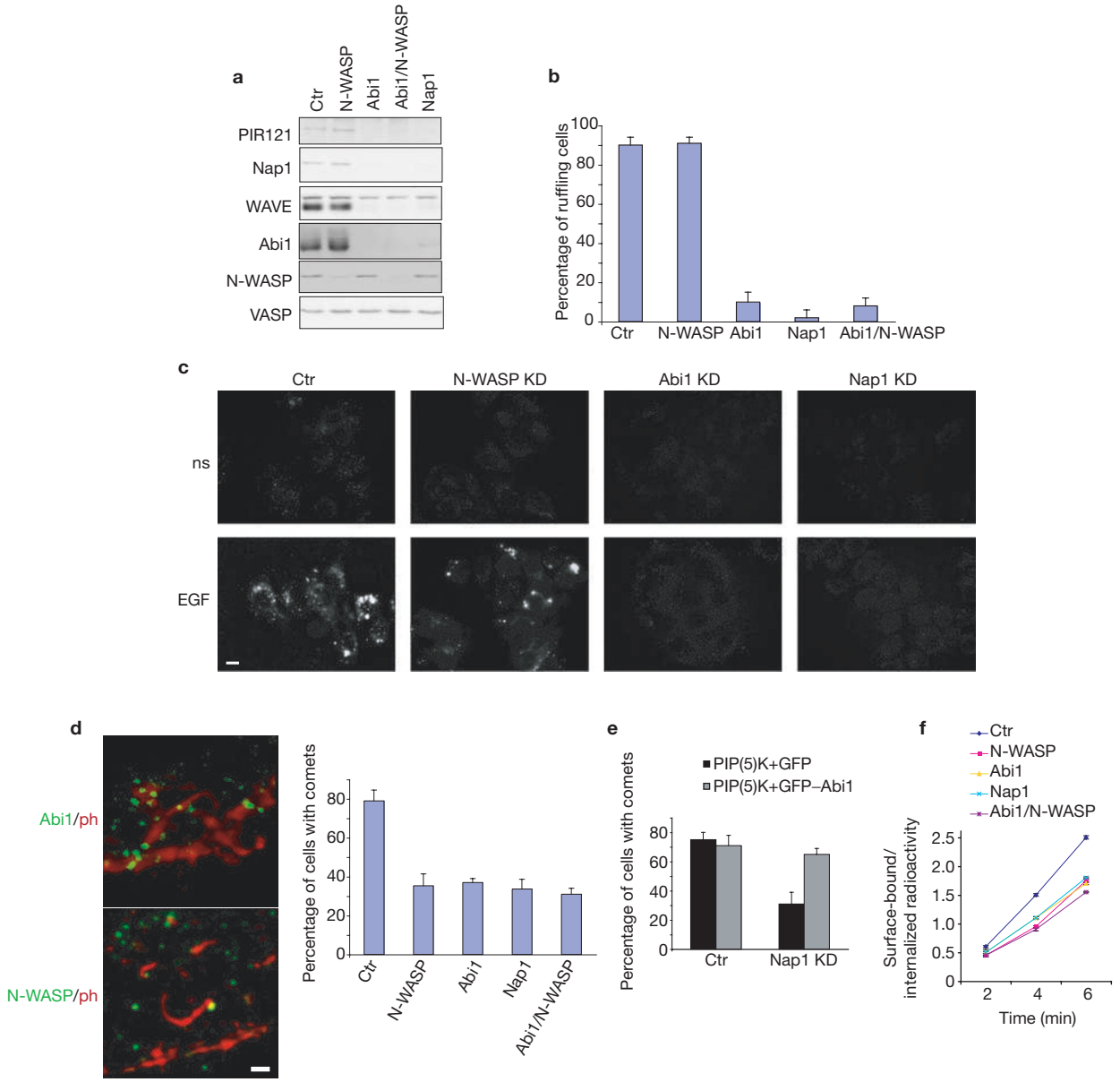

Figure 2 Abi1 is implicated in ruffle formation and macropinocytosis through WAVE, and vesicle rocketing and EGFR endocytosis through N-WASP. (**a**) Generation of HeLa stable knockdown cells. Immunoblot analysis (indicated on the left) of WAVE, Nap1, PIR121, Abi1 and N-WASP in the various HeLa knockdown cells (indicated on top) obtained as described in the Methods. VASP levels were used as a loading control. (**b**) The WAVE–Abi1–Nap1–PIR121 complex, but not N-WASP, is essential for EGF-induced ruffling. HeLa cells stimulated or not with EGF (100 ng ml^{-1}) were fixed and stained with rhodamine-conjugated phalloidin to detect F-actin (data not shown). The percentage (mean ± s.e.m.) of ruffling cells was determined. (**c**) The WAVE–Abi1–Nap1–PIR121 complex, but not N-WASP, mediates macropinocytosis. HeLa cells incubated (30 min) with rhodamine-conjugated dextran (M_r 70K) in the presence (EGF) or absence (ns) of EGF were washed and fixed. Scale bar, 10 µm. For quantification see Supplementary Information, Table S1. KD, knocked down. (**d**) Removal of N-WASP, Abi1 or Nap1 impairs PIP(5)K-induced actin tail formation. Left: Abi1 and N-WASP localize at the tip of PIP(5)K-induced actin tails. HeLa cells were cotransfected with GFP–Abi1 (Abi1) or GFP–N-WASP (N-WASP) together with Myc-tagged PIP(5)K, fixed and processed to visualize GFP proteins (green), and stained with phalloidin (ph) or anti-Myc to detect F-actin (red) or PIP(5)K (data not shown) (see Supplementary Information, Fig. S2 and Movie S1). Scale bar, 1 µm. Right: quantification of actin tail formation. HeLa cells in which the expression of N-WASP, Abi1, Nap1, or N-WASP and Abi1 was knocked down, or control cells (ctr), were transfected with Myc–PIP(5)K, fixed and stained as in **a**. The percentage (mean ± s.e.m.) of PIP(5)K-expressing cells showing at least one actin tail is reported. (**e**) Reconstitution of Abi1 expression in Nap1-knockdown cells is sufficient to restore efficient comet tail formation. Control HeLa and Nap1 knockdown cells were transfected with Myc-tagged PIP(5)K together with empty GFP (PIP(5)K + GFP) or GFP–Abi1 (PIP(5)K + GFP–Abi1). The percentage of PIP(5)K-positive cells displaying actin tails was determined as described in **d**. (**f**) Initial rate of EGFR internalization. HeLa cells were incubated with ^{125}I-labelled EGF (1.5 ng ml^{-1}) for the indicated times at 37 °C, and surface-bound and internalized radioactivity was determined as in ref. 43. The mean ± s.e.m. of independent triplicates is shown.

The high-affinity binding of Abi1 to N-WASP *in vitro* suggested that this interaction might be physiologically relevant. This was verified by *in vivo* experiments as follows. Ectopically expressed Myc-tagged N-WASP and HA-tagged Abi1 could associate in reciprocal co-immunoprecipitation experiments (Fig. 1d). More importantly, endogenous N-WASP could be recovered onto Abi1 immunoprecipitates obtained

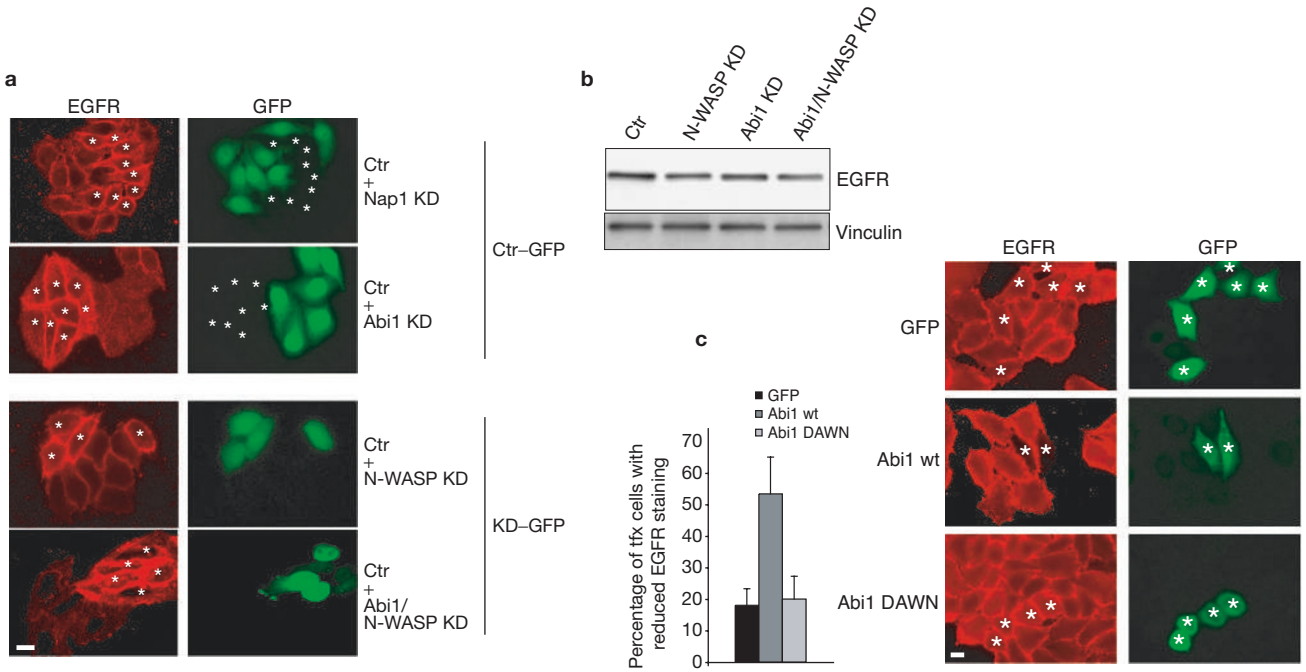

Figure 3 Removal of Abi1 or N-WASP increases EGFR at the cell surface. (**a**) Ablation of Nap1, Abi1, N-WASP, or Abi1 and N-WASP increases cell-surface EGFR. Control HeLa cells, expressing lentivirus-driven GFP (ctr–GFP), were mixed with Nap1- (ctr + Nap1 KD) or Abi1- (ctr + Abi1 KD) ablated cells obtained as described in the Methods. Alternatively, control HeLa cells, infected with empty pSuper-based vectors, were mixed with N-WASP- (ctr + N-WASP KD) or N-WASP- and Abi1-ablated (ctr + Abi1/N-WASP KD) cells expressing GFP (KD–GFP). Cells were then fixed, and anti-EGFR antibodies that recognize an extracellular epitope were used prior to permeabilization to detect cell-surface EGFR. The GFP epifluorescence enabled control (ctr–GFP positive) to be distinguished from knockdown cells in the Abi1 and Nap1 cases (upper panels). Conversely, N-WASP knockdown and Abi1/N-WASP knockdown, but not wild-type cells, were GFP positives (lower panels). Notably, EGF treatment of wild-type or knockdown cells caused a reduction of cell-surface EGFR as a consequence of internalization (data not shown). Asterisks mark knockdown cells in all cases. Scale bar, 10 μm. (**b**) Abi1, Nap1, N-WASP and Abi1/N-WASP knockdown cells show comparable levels of total EGFR. Equal amounts of total cellular lysates from control (ctr), N-WASP knockdown, Abi1 knockdown, N-WASP and Abi1 knockdown (Abi1/N-WASP KD) cells were immunoblotted with anti-EGFR or anti-vinculin (loading control) antibodies. (**c**) Expression of Abi1 in Nap1 knockdown cells reduces cell-surface EGFR. Right: Nap1 knockdown cells were transfected with wild-type GFP–Abi1 (Abi1 wt), GFP–Abi1 DAWN (Abi1 DAWN), a mutant impaired in the SH3 domain[21], or with empty vector (GFP). Cells were fixed and stained as in **a**. Scale bar, 10 μm. Left: the percentage of transfected cells that showed a reduction in cell-surface EGFR signal is reported. Data are expressed as the mean ± s.e.m. of three independent experiments.

from lysates of HeLa cells (Fig. 1e). Notably, Abi1 immunoprecipitates also contained WAVE, as previously shown[11,12,15], suggesting that Abi1 may regulate/integrate the activities of the two major nucleation promoting factors (NPFs), N-WASP and WAVE. Only a small fraction of total N-WASP, compared with the majority of WAVE (more than 90%), was found bound to Abi1 (Fig. 1e), supporting the existence of two distinct Abi1-based, NPF-containing complexes. Consistently, no N-WASP could be detected in WAVE immunoprecipitates, which contained Abi1 (see Supplementary Information, Fig. S1c). Additionally, Abi1, but not WAVE, was present in N-WASP immunoprecipitates obtained from N-WASP knockout cells stably re-expressing Flag-tagged N-WASP (Fig. 1f). Finally, in gel filtration experiments, Abi1 perfectly co-eluted with WAVE, whereas it only partially cofractionated with N-WASP, indicating that Abi1 and N-WASP form a complex of relatively low abundance, distinct from that containing WAVE or other known Abi1 interactors, such as Sos-1 or Eps8 (see Supplementary Information, Fig. S1d). Thus, Abi1 is a physiological and direct interactor of N-WASP and a potent inducer of its activity.

The finding that Abi1 can interact with WAVE through its N-terminal region, and with N-WASP through its SH3 domain, indicates that this adaptor may use its different domains to integrate or functionally specify the activity of the major NPFs in cells. To explore these possibilities, a molecular genetic approach that exploits RNAi-based technology was used to generate cells in which the expression of either the entire WAVE-based complex or N-WASP was ablated. To this end, Abi1 and N-WASP were individually or simultaneously knocked down in HeLa cells (Fig. 2a). As an additional control, we also generated cells in which Nap1 was silenced. As previously reported, RNAi-mediated removal of Abi1 or Nap1 also led to the degradation of all the other subunits of the WAVE–Abi1–Nap1–PIR121 complex, leaving the expression levels of N-WASP unaltered (Fig. 2a). Conversely, N-WASP interference by RNAi did not affect the protein levels of Abi1, WAVE, Nap1 and PIR121 (Fig. 2a). Notably, the simultaneous interference of Abi1 and N-WASP led to the silencing or degradation of both N-WASP and the WAVE-based complex (Fig. 2a).

Active N-WASP has been localized to membrane protrusions by live fluorescence resonance energy transfer (FRET) analysis[18]. Additionally, the WAVE–Abi1–Nap1–PIR121 complex was shown to be essential for initiating Arp2/3-dependent, site-directed polymerization at the leading edge of lamellipodia. This suggests that at this site Abi1 may integrate the activity of both WAVE and N-WASP. To test this, membrane ruffling in response to EGF stimulation was monitored in the various knockdown cells. Removal of the WAVE–Abi1–Nap1–PIR121 complex by knocking down either Abi1 or Nap1 strongly diminished EGF-induced ruffles (Fig. 2b and data not shown). Conversely, no inhibition could be observed upon removal of N-WASP (Fig. 2b), in agreement with the observation

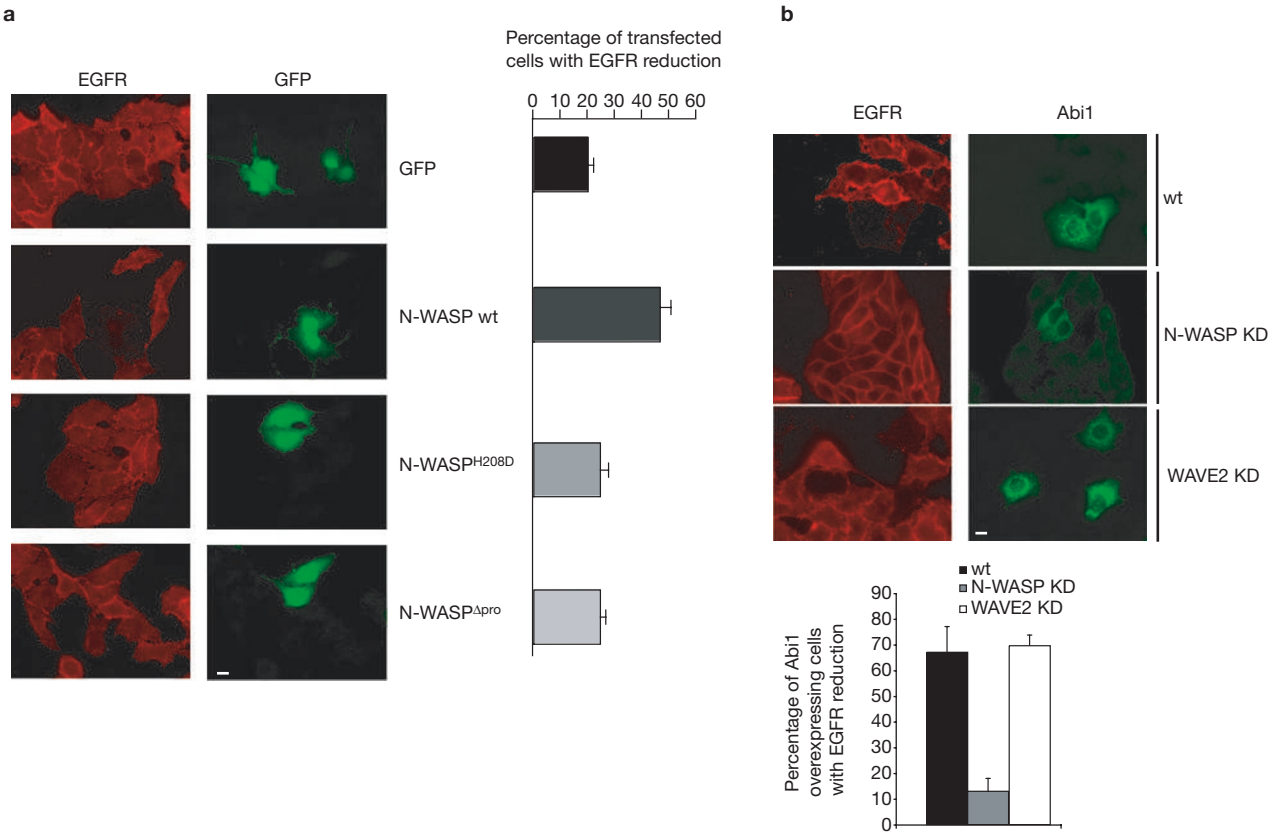

Figure 4 The overexpression of either N-WASP or Abi1 decreases cell-surface EGFR. (**a**) Structure–function analysis of N-WASP on the distribution of cell-surface EGFR. HeLa cells were transfected with GFP, GFP–N-WASP, GFP–N-WASP^{H208D} (ref. 24) (a mutant unable to bind to Cdc42), or GFP–N-WASP$^{\Delta pro}$, a mutant lacking the entire proline-rich region[24]. Serum-starved cells were then fixed and stained with anti-EGFR (EGFR) as described in Fig. 3a, or processed for epifluorescence (GFP) to detect transfected cells. Scale bar, 10 μm. (**b**) Abi1 expression reduces cell-surface EGFR in wild-type and WAVE2 knockdown (KD) cells, but not in N-WASP knockdown HeLa cells. Control (wt), N-WASP knockdown or WAVE2 knockdown HeLa cells were transfected with HA-tagged Abi1, fixed and stained as described above to detect cell-surface EGFR (EGFR), and subsequently with anti-polyclonal HA antibodies to identify transfected (Abi1) cells. Scale bar, 10 μm. The percentage of transfected cells that showed a reduction in their cell-surface EGFR signal is reported in the graph (right). Data are expressed as the mean ± s.e.m. of three independent experiments.

that genetic ablation of N-WASP in fibroblasts had no effect on lamellipodia formation[23,24]. Further support for the notion that the activities of WAVE and N-WASP are independent came from the observation that EGF-induced macropinocytosis, which has been functionally coupled to Rac activity, actin remodelling and WAVE functions[14], was reduced upon removal of the WAVE–Abi1–Nap1–PIR121 complex (Abi1 and Nap1 knockdown cells), but unaffected by N-WASP ablation (Fig. 2c).

N-WASP is essential for actin-based motility of different pathogens, such as *Shigella flexneri* or Vaccinia virus[23,24]. Upon invasion, these pathogens hijack the host machinery that is used for actin polymerization, inducing the formation of actin comet tails to drive their movements. This process mimics the naturally occurring N-WASP-mediated rocketing of endomembrane-derived vesicles[25], which is enhanced in mammalian cells by the expression of the lipid kinase phosphatidylinositol-4-phosphate-5-kinase (PIP(5)K), leading to the generation of PtdIns(4,5)P_2-rich endomembranes[26]. Analysis of the cellular localization of Abi1 revealed that it is specifically recruited to the surface of PtdIns(4,5)P_2-induced rocketing vesicles in HeLa cells and a variety of different cell lines, displaying a pattern that overlaps with that of N-WASP (Fig. 2d and Supplementary Information, Fig. S2a–c and Movie S1a). Notably, no WAVE proteins were detected in these structures (see Supplementary Information, Fig. S2a), suggesting that localization at specific intracellular sites of different Abi1–NPF pools may dictate their functional roles. Consistently, individual removal of N-WASP or Abi1 significantly impaired the formation of actin tails induced by PIP(5)K (Fig. 2d). A similar impairment could also be observed upon Nap1 removal (Fig. 2d), which leads to degradation of Abi1, in addition to WAVE and PIR121 (Fig. 2a). However, ectopic re-expression of Abi1 in these cells was sufficient to restore PIP(5)K-induced comet tail formation (Fig. 2e), but not EGF-induced ruffling (data not shown). Thus, the Abi1–N-WASP, but not the WAVE–Abi1–Nap1–PIR121 complex, whose stability could not be rescued by Abi1 expression, is sufficient for optimum vesicle motility. Notably, this WAVE-independent activity of Abi1 is conserved throughout evolution; in *Drosophila*, bristle formation is independent of WAVE, but dependent on Abi1/WASP (Bogdan *et al.*[27], accompanying manuscript).

In addition to vesicular transport, WASP and N-WASP, and their yeast homologue Las17, have been implicated in endocytosis of membrane receptors[28,29]. In mammals, endocytosis of membrane receptors, such as EGF and transferrin receptors, proceeds mainly through the formation of clathrin-coated pits (CCPs) and vesicles[30]. Direct visualization of the recruitment of actin and N-WASP accompanying the internalization of single CCPs can only be obtained by using two-colour total internal reflection fluorescence (TIRF) microscopy[31–33]. Using a similar approach, we found that Abi1, but not WAVE2 (ref. 33), could be specifically recruited to these sites (see Supplementary Information, Fig. S2d

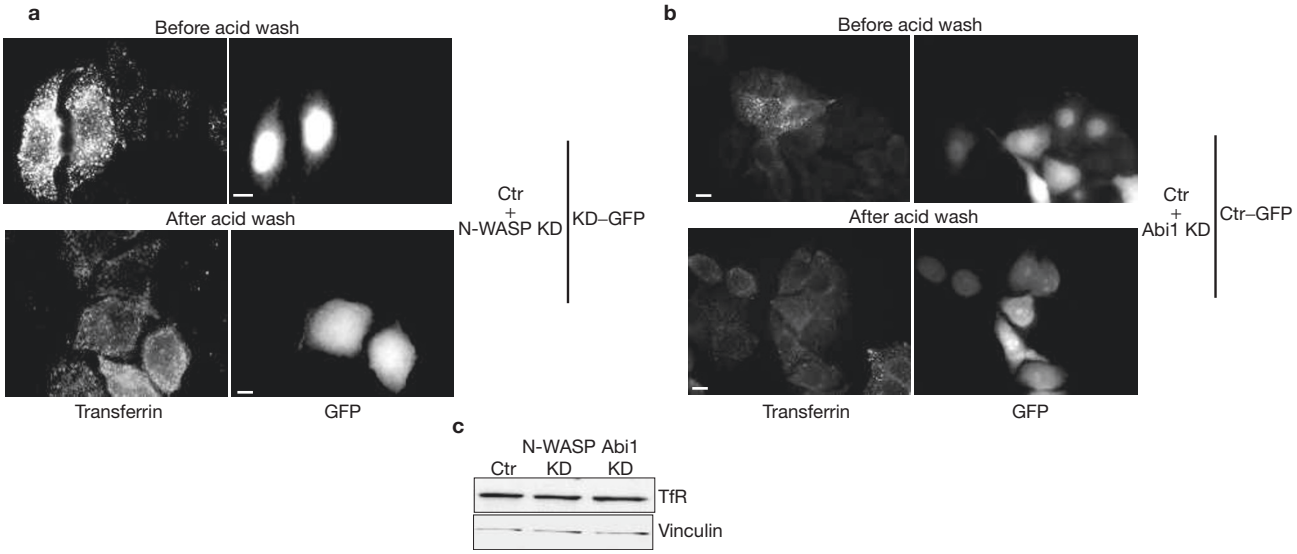

Figure 5 Removal of Abi1 or N-WASP increases TfR at the cell surface. (**a**) Removal of N-WASP increases cell-surface-associated transferrin. Control HeLa cells, infected with the appropriate empty vector, were mixed with N-WASP-ablated cells (ctr + N-WASP KD) expressing GFP (KD–GFP). (**b**) Removal of Abi1 increases cell-surface-associated transferrin. Control HeLa cells, expressing lentivirus-driven GFP (ctr–GFP), were mixed with Abi1-ablated cells (ctr + Abi1 KD) obtained as described in the Methods. In **a** and **b**, cells were incubated with rhodamine-conjugated transferrin for 15 min and either washed with PBS (before acid wash) or with ice-cold 0.2 M acetic acid (pH 2.8) containing 0.5 M NaCl for 5 min (after acid wash), then fixed and stained. Washing with acid strips transferrin that is bound to cell-surface receptors. Scale bars, 10 μm. (**c**) Abi1 and N-WASP knockdown cells show comparable levels of total TfR. Equal amounts of total cellular lysates from control (ctr), N-WASP knockdown, and Abi1 knockdown cells were immunoblotted with the indicated antibodies.

and Movie S2). More importantly, ectopically expressed Abi1 and N-WASP extensively colocalized at the cell surface in spots whose lateral mobility — which has been shown to frequently accompany the pinching off of vesicles[31,34,35] — was significantly increased (see Supplementary Information, Movie S2). Remarkably, the lateral motility of Abi1- and N-WASP-containing spots on the plasma membrane was strictly dependent on actin dynamics, because no such movements were detected in the presence of the G-actin-sequestering drug, Latrunculin A (see Supplementary Information, Movie S3). Collectively, these observations suggest a site-specific functional role exerted by Abi1 and N-WASP in mediating actin-dependent endocytic events. Accordingly, individual removal of either Abi1 or N-WASP caused a comparable reduction in the initial rate of internalization of EGFR (Fig. 2f), which relies on clathrin-mediated uptake[30]. Moreover, concomitant silencing of Abi1 and N-WASP did not cause any worsening of the phenotype, providing genetic evidence that these proteins act in the same signalling cascade (Fig. 2f). Thus Abi1 critically modulates N-WASP/Arp2/3-stimulated actin polymerization in clathrin-mediated endocytosis.

The expression of membrane receptors, such as EGFR and TfR, at the cell surface depends on the rates of protein synthesis and protein degradation, and on endocytic transport[36]. The involvement of Abi1 and N-WASP in endocytosis and vesicular transport prompted us to look at the distribution of cell-surface EGFR and TfR. EGFR and TfR are considered to be the prototypes of ligand-induced and constitutive internalization, respectively[30]. Individual removal of N-WASP, Abi1, or Nap1 significantly increased the amount of EGFR at the plasma membrane (Fig. 3a), as revealed by staining, prior to permeabilization, of cell-surface receptors with an antibody that recognizes the extracellular portion of the EGFR. Notably, the total steady-state levels of EGFR were not affected in the various knockdown cells (Fig. 3b). Most importantly, the expression of Abi1, but not of a mutant impaired in the SH3 domain[21] nor of WAVE2 (see Supplementary Information, Fig. S3a), significantly lowered the amounts of cell-surface EGFR in Nap1-knockdown cells (Fig. 3c). Moreover, the transient transfection of Abi1 in Nap1 knockdown cells was not sufficient to restore WAVE expression (see Supplementary Information, Fig. S3b). Finally, no effect on cell-surface levels of EGFR (or TfR; see below) were observed following the expression of a mutant of WAVE2 that lacked the verprolin homology domain (ΔVPH-WAVE2) and was shown to act as a dominant negative[37] (see Supplementary Information, Fig. S4a, b). Together, these results emphasize the relevance and specificity of the Abi1–N-WASP complex, but not of the WAVE complex in regulating EGFR cellular distribution. Additional evidence was obtained by ectopically expressing Abi1 or N-WASP in wild-type HeLa cells. Under these conditions, the levels of cell-surface EGFR were significantly reduced (the opposite is observed following RNAi-mediated ablation of the same proteins), indicating that Abi1 and N-WASP are limiting factors in this process (Fig. 4a). The effect of Abi1 was entirely dependent on N-WASP, but not on WAVE, because ectopic expression of Abi1 failed to decrease EGFR at the surface of N-WASP-knockdown cells, but not of WAVE2- knockdown cells (Fig. 4b). Moreover, a mutant of Abi1 no longer able to associate with WAVE2, but retaining the N-WASP-binding capability, was as efficient as wild-type Abi1 in decreasing cell-surface EGFR (see Supplementary Information, Fig. S4c).

Similarly, individual ablation of either N-WASP or Abi1 increased the intensity of the rhodamine-conjugated transferrin signal. Notably, most of the signal derived from the cell surface, as it could be removed by acidic washes prior to fixation (Fig. 5a, b). Hence, the levels of cell-surface TfR, but not the total TfR (Fig. 5c), were significantly affected by interference with either Abi1 and/or N-WASP.

Often, concomitant signalling events are needed to optimally regulate, *in vivo* and *in vitro,* N-WASP-mediated actin dynamics. Accordingly, full-length N-WASP, but not N-WASP mutants impaired in either Cdc42

(H208D) or in SH3 (Δpro) binding sites, reduced cell-surface EGFR (Fig. 4a). Additionally, Cdc42 and Abi1 synergistically activated N-WASP *in vitro* (Fig. 1c). Thus, multiple signalling events probably contribute to specifying the functional role of the Abi1–N-WASP complex.

In summary, we showed that Abi1 is a critical N-WASP modulator during endocytosis and vesicular transport. Notably, Abi1 is also an essential component and regulator of the WAVE-based complex acting downstream of Rac. Interestingly, this dual regulation of N-WASP and WAVE by Abi1 appears to be conserved throughout evolution, being documented also in *Drosophila*[19,38]. Thus, Abi1 seems to sit at the heart of a multilayered system of regulation for the actin cytoskeleton, raising the interesting possibility that by entering N-WASP- and/or WAVE-based protein complexes, it may functionally orchestrate the activities of these two major nucleation promoting factors within cells. As a result, it may contribute to specifying WAVE and N-WASP functions in actin-dynamics-based membrane protrusion and intracellular transport, respectively. □

METHODS

Expression vectors. HA-tagged Abi1, wild-type EGFP–Abi1, EGFP–Abi1–DAWN (a mutant impaired in the SH3 domain), and EYFP-Abi1 or EYFP-ΔN-Abi1 plasmids were previously described[21]. Bovine Myc-tagged N-WASP was provided by M. Kirschner. Myc-tagged PIP(5)K was a gift from L. Machesky. EGFP-tagged wild-type N-WASP, N-WASP^{H208D} and N-WASP$^{\Delta pro}$ vectors were described in ref. 24. Human Flag-tagged ΔVPH WAVE2 was a gift from T. Takenawa.

Antibodies. Anti-HA-11, anti-Myc 9E10, anti-His, anti-Abi1, anti-WAVE, anti-Nap1 and anti-PIR121 antibodies were described in ref. 11. Anti-N-WASP was kindly provided by T. Takenawa. Monoclonal anti-vinculin and anti-VASP were from Transduction Laboratories (Lexington, KY). Anti-EGFR (Ab-1) was from Oncogene Research Products (Cambridge, MA). Polyclonal anti-HA was from Santa Cruz (Santa Cruz, CA). Monoclonal anti-Flag and anti-Tubulin β were from Sigma (St Louis, MO). TfR antibodies were from Zymed (San Francisco, CA). Rhodamine-conjugated EGF and transferrin were from Molecular Probes (Eugene, OR).

Recombinant proteins. Full-length Abi1, the isolated SH3 domain of Abi1, Cdc42 and Rac1 were produced as GST fusion proteins in *Escherichia coli* as described[11]. Full-length Grb2 and its SH3 domain were produced as described[20]. Actin was isolated from rabbit muscles and purified in the Ca-ATP–G-actin form by Sephadex G-200 chromatography in G buffer (5 mM Tris–HCl at pH 7.8, 0.1 mM $CaCl_2$, 0.2 mM ATP, 1 mM dithiothreitol and 0.01% NaN_3)[39]. Actin was fluorescently labelled with pyrenyl-iodoacetamide[39]. Human His–N-WASP was expressed in Sf9 cells[40]. The C-terminal domain (VCA) of human N-WASP was expressed as a recombinant GST fusion protein and separated from GST by proteolytic cleavage[41]. The Arp2/3 complex was purified from bovine brain[39]. The proline-rich peptide used to inhibit the interaction between Abi1 and N-WASP was previously described[20,21].

Generation of HeLa-knockdown cells. Abi1- and WAVE2-knockdown cells were generated as described in ref. 11. Nap1-knockdown cells were obtained by infection with pSuper-Retro-puro-Nap1 (ref. 15), and single clones were isolated. Three selected clones were further characterized for their expression of Nap1 and the components of the WAVE–Abi1–Nap1–PIR121 complex, and for their lack of ruffling in response to EGF. Similar results were obtained with all the clones analysed. All the subsequent experiments were then performed with one of the isolated clones. N-WASP knockdown was obtained by infecting Abi1 knockdown or control HeLa cells twice with an shRNA-expressing pLL3.7 lentivirus[42]. This enabled 100% efficiency of infection. Attempts to isolate single clones with complete N-WASP protein depletion failed repeatedly. All the experiments were thus performed on the resulting mass population. N-WASP downregulation was determined by immunoblot analysis (Fig. 2a).

Actin polymerization assays. Actin polymerization was monitored by the increase in fluorescence of 10% pyrenyl-labelled actin. Polymerization was induced by addition of KCl (0.1 M), $MgCl_2$ (1 mM) and EGTA (0.2 mM) to a solution of Ca-ATP–G-actin containing Arp2/3 and the different proteins as described in Fig. 1. Fluorescence measurements were performed at 20 °C in a Safax flx spectrofluorometer in which polymerization time courses of up to 10 samples can be monitored simultaneously[11]. Addition of Abi1 to pyrenyl–actin and Arp2/3 had no effect on actin polymerization (data not shown and ref. 11). The affinities of Abi1, Cdc42 or SH3 domain were derived from analysis of the dependence of the maximal rate of actin polymerization on ligand concentration as described[20].

Transfection, immunofluorescence microscopy and cell biological assays. Cells seeded on gelatin were transfected with the indicated expression vectors using FuGene (Invitrogen, Carlsbad, CA) according to the manufacturer's instructions. After 24 h, cells were processed for epifluorescence or indirect immunofluorescence microscopy. Briefly, cells were fixed in 4% paraformaldehyde for 10 min, permeabilized in 0.1% Triton X-100 and 0.2% BSA for 10 min, and then incubated with the primary antibody for 45 min, followed by incubation with the secondary antibody for 30 min. F-actin was detected by staining with phalloidin (Molecular Probes) at a concentration of 6.7 U ml^{-1}.

The formation of EGF-induced ruffling was monitored as described[11]. The initial rate of EGFR endocytosis was determined as described[43]. PIP(5)K-induced comets were determined as described[17]. *In vitro* binding, co-immunoprecipitation and gel filtration experiments were as described[11].

BIND identifiers. Six BIND identifiers (www.bind.ca) are associated with this manuscript: 331009, 331010, 331011, 331012, 331013 and 331014.

Note: Supplementary Information is available on the Nature Cell Biology website.

ACKNOWLEDGEMENTS

This work was supported by grants from: Associazione Italiana Ricerca sul Cancro (AIRC) and AIRC Regionale Lombardia to G.S.; Human Science Frontier Program to G.S. and M.F.C. (grant number RGP0072/2003-C); the Italian Ministry of Health (grant R.F. 02/184) to G.S.; the French Ligue Nationale Contre le Cancer to M.F.C. ('équipe labellisée Ligue'); the Fondazione Italiana Ricerca sul Cancro (FIRC) to M.I.; European Community (VI Framework) to G.S.; EMBO to M.H.; and from the Deutsche Forschungsgemeinschaft (DFG) (SPP 1150) to K.R. and T.E.B.S. We would like to thank M. Garre and S. Bossi for technical help, and S. Lommel for providing N-WASP constructs.

COMPETING FINANCIAL INTERESTS

The authors declare that they have no competing financial interests.

Published online at http://www.nature.com/naturecellbiology/
Reprints and permissions information is available online at http://npg.nature.com/reprintsandpermissions/

1. Pantaloni, D., Le Clainche, C. & Carlier, M. F. Mechanism of actin-based motility. *Science* **292,** 1502–1506 (2001).
2. Pollard, T. D. & Borisy, G. G. Cellular motility driven by assembly and disassembly of actin filaments. *Cell* **112,** 453–465 (2003).
3. Qualmann, B. & Kessels, M. M. Endocytosis and the cytoskeleton. *Int. Rev. Cytol.* **220,** 93–144 (2002).
4. Takenawa, T. & Miki, H. WASP and WAVE family proteins: key molecules for rapid rearrangement of cortical actin filaments and cell movement. *J. Cell Sci.* **114,** 1801–1809 (2001).
5. Moreau, V. *et al.* A complex of N-WASP and WIP integrates signalling cascades that lead to actin polymerization. *Nature Cell Biol.* **2,** 441–448 (2000).
6. Stradal, T. E. *et al.* Regulation of actin dynamics by WASP and WAVE family proteins. *Trends Cell Biol.* **14,** 303–311 (2004).
7. Kitamura, T. *et al.* Molecular cloning of p125Nap1, a protein that associates with an SH3 domain of Nck. *Biochem. Biophys. Res. Commun.* **219,** 509–514 (1996).
8. Kobayashi, K. *et al.* p140Sra-1 (specifically Rac1-associated protein) is a novel specific target for Rac1 small GTPase. *J. Biol. Chem.* **273,** 291–295 (1998).
9. Eden, S., Rohatgi, R., Podtelejnikov, A. V., Mann, M. & Kirschner, M. W. Mechanism of regulation of WAVE1-induced actin nucleation by Rac1 and Nck. *Nature* **418,** 790–793 (2002).
10. Shi, Y., Alin, K. & Goff, S. P. Abl-interactor-1, a novel SH3 protein binding to the carboxy-terminal portion of the Abl protein, suppresses v-abl transforming activity. *Genes Dev.* **9,** 2583–2597 (1995).
11. Innocenti, M. *et al.* Abi1 is essential for the formation and activation of a WAVE2 signalling complex. *Nature Cell Biol.* **6,** 319–327 (2004).
12. Gautreau, A. *et al.* Purification and architecture of the ubiquitous Wave complex. *Proc. Natl Acad. Sci. USA* **101,** 4379–4383 (2004).
13. Parsons, M. *et al.* Spatially distinct binding of Cdc42 to PAK1 and N-WASP in breast carcinoma cells. *Mol. Cell Biol.* **25,** 1680–1695 (2005).
14. Suetsugu, S., Yamazaki, D., Kurisu, S. & Takenawa, T. Differential roles of WAVE1 and WAVE2 in dorsal and peripheral ruffle formation for fibroblast cell migration. *Dev. Cell* **5,** 595–609 (2003).

15. Steffen, A. *et al.* Sra-1 and Nap1 link Rac to actin assembly driving lamellipodia formation. *EMBO J.* **23,** 749–759 (2004).
16. Innocenti, M. *et al.* Phosphoinositide 3-kinase activates Rac by entering in a complex with Eps8, Abi1, and Sos-1. *J. Cell Biol.* **160,** 17–23 (2003).
17. Disanza, A. *et al.* Eps8 controls actin-based motility by capping the barbed ends of actin filaments. *Nature Cell Biol.* **6,** 1180–1188 (2004).
18. Lorenz, M., Yamaguchi, H., Wang, Y., Singer, R. H. & Condeelis, J. Imaging sites of N-Wasp activity in lamellipodia and invadopodia of carcinoma cells. *Curr. Biol.* **14,** 697–703 (2004).
19. Bogdan, S. & Klambt, C. Kette regulates actin dynamics and genetically interacts with Wave and Wasp. *Development* **130,** 4427–4437 (2003).
20. Carlier, M. F. *et al.* GRB2 links signaling to actin assembly by enhancing interaction of neural Wiskott-Aldrich syndrome protein (N-WASp) with actin-related protein (ARP2/3) complex. *J. Biol. Chem.* **275,** 21946–21952 (2000).
21. Innocenti, M. *et al.* Mechanisms through which Sos-1 coordinates the activation of Ras and Rac. *J. Cell Biol.* **156,** 125–136 (2002).
22. Fukuoka, M. *et al.* A novel neural Wiskott-Aldrich syndrome protein (N-WASP) binding protein, WISH, induces Arp2/3 complex activation independent of Cdc42. *J. Cell Biol.* **152,** 471–482 (2001).
23. Snapper, S. B. *et al.* N-WASP deficiency reveals distinct pathways for cell surface projections and microbial actin-based motility. *Nature Cell Biol.* **3,** 897–904 (2001).
24. Lommel, S. *et al.* Actin pedestal formation by enteropathogenic *Escherichia coli* and intracellular motility of *Shigella flexneri* are abolished in N-WASP-defective cells. *EMBO Rep.* **2,** 850–857 (2001).
25. Taunton, J. Actin filament nucleation by endosomes, lysosomes and secretory vesicles. *Curr. Opin. Cell Biol.* **13,** 85–91 (2001).
26. Rozelle, A. L. *et al.* Phosphatidylinositol 4,5-bisphosphate induces actin-based movement of raft-enriched vesicles through WASP-Arp2/3. *Curr. Biol.* **10,** 311–320 (2000).
27. Bogdan, S., Stephan, R., Löbke, C., Mertens, A. & Klämbt, C. Abi activates WASP to promote sensory organ development. *Nature Cell Biol.* **7,** DOI: 10.1038/ncb1305 (2005).
28. Kessels, M. M. & Qualmann, B. Syndapins integrate N-WASP in receptor-mediated endocytosis. *EMBO J.* **21,** 6083–6094 (2002).
29. Naqvi, S. N., Zahn, R., Mitchell, D. A., Stevenson, B. J. & Munn, A. L. The WASp homologue Las17p functions with the WIP homologue End5p/verprolin and is essential for endocytosis in yeast. *Curr. Biol.* **8,** 959–962 (1998).
30. Conner, S. D. & Schmid, S. L. Regulated portals of entry into the cell. *Nature* **422,** 37–44 (2003).
31. Merrifield, C. J., Feldman, M. E., Wan, L. & Almers, W. Imaging actin and dynamin recruitment during invagination of single clathrin-coated pits. *Nature Cell Biol.* **4,** 691–698 (2002).
32. Merrifield, C. J., Qualmann, B., Kessels, M. M. & Almers, W. Neural Wiskott Aldrich Syndrome Protein (N-WASP) and the Arp2/3 complex are recruited to sites of clathrin-mediated endocytosis in cultured fibroblasts. *Eur. J. Cell Biol.* **83,** 13–18 (2004).
33. Benesch, S. *et al.* N-WASP deficiency impairs EGF internalization and actin assembly at clathrin-coated pits. *J. Cell Sci.* **118,** 3103–3115 (2005).
34. Yarar, D., Waterman-Storer, C. M. & Schmid, S. L. A dynamic actin cytoskeleton functions at multiple stages of clathrin-mediated endocytosis. *Mol. Biol. Cell* **16,** 964–975 (2005).
35. Merrifield, C. J., Perrais, D. & Zenisek, D. Coupling between clathrin-coated-pit invagination, cortactin recruitment, and membrane scission observed in live cells. *Cell* **121,** 593–606 (2005).
36. Wiley, H. S. Trafficking of the ErbB receptors and its influence on signaling. *Exp. Cell Res.* **284,** 78–88 (2003).
37. Suetsugu, S., Miki, H. & Takenawa, T. Identification of two human WAVE/SCAR homologues as general actin regulatory molecules which associate with the Arp2/3 complex. *Biochem. Biophys. Res. Commun.* **260,** 296–302 (1999).
38. Kunda, P., Craig, G., Dominguez, V. & Baum, B. Abi, Sra1, and Kette control the stability and localization of SCAR/WAVE to regulate the formation of actin-based protrusions. *Curr. Biol.* **13,** 1867–1875 (2003).
39. Pantaloni, D., Boujemaa, R., Didry, D., Gounon, P. & Carlier, M. F. The Arp2/3 complex branches filament barbed ends: functional antagonism with capping proteins. *Nature Cell Biol.* **2,** 385–391 (2000).
40. Loisel, T. P., Boujemaa, R., Pantaloni, D. & Carlier, M. F. Reconstitution of actin-based motility of *Listeria* and *Shigella* using pure proteins. *Nature* **401,** 613–616 (1999).
41. Egile, C. *et al.* Activation of the CDC42 effector N-WASP by the *Shigella flexneri* IcsA protein promotes actin nucleation by Arp2/3 complex and bacterial actin-based motility. *J. Cell Biol.* **146,** 1319–1332 (1999).
42. Rubinson, D. A. *et al.* A lentivirus-based system to functionally silence genes in primary mammalian cells, stem cells and transgenic mice by RNA interference. *Nature Genet.* **33,** 401–406 (2003).
43. Haglund, K. *et al.* Multiple monoubiquitination of RTKs is sufficient for their endocytosis and degradation. *Nature Cell Biol.* **5,** 461–466 (2003).

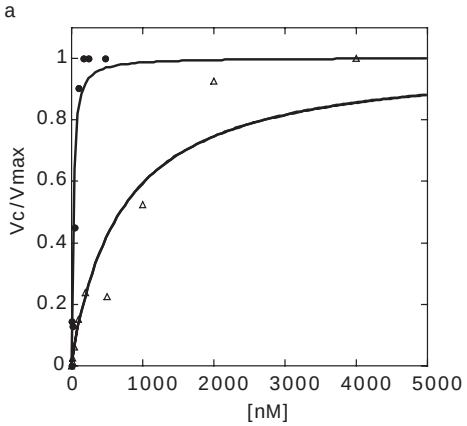

Abi1	Abi1 SH3	Grb2	Grb2 SH3
15	680	115	590

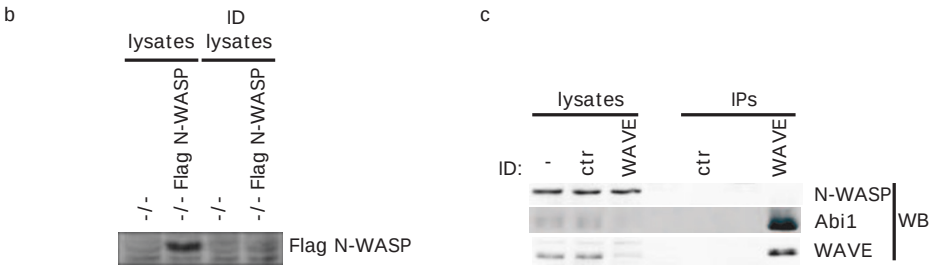

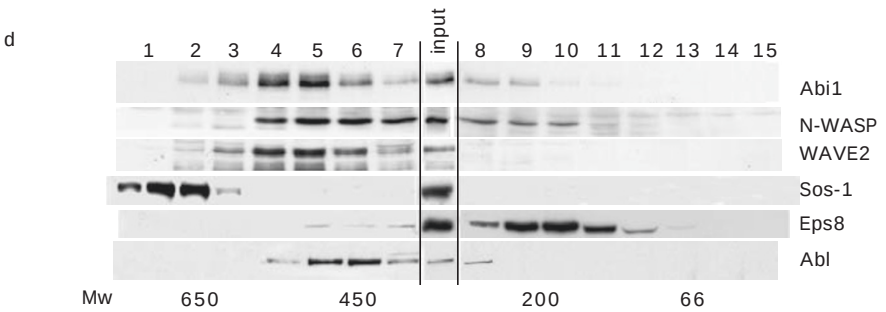

Figure S1a Concentration dependence of N-WASP stimulation by Abi1 or its SH3 domain, or by Grb2 or its N-terminal SH3 domain. Arp2/3-mediated actin polymerization of N-WASP (30 nM) in the presence of increasing concentrations of Abi1 (closed circles) or its SH3 domain (open triangles). Data are expressed as the ratio between maximal activation (Vmax) and the activation observed at each concentration used (Vc). The concentrations of Abi1, its SH3 domain, Grb2 and its N-terminal SH3 domain leading to half-maximal effect are indicated on the right. S1b. Expression of Flag-tagged N-WASP in N-WASP null fibroblasts. N-WASP null fibroblasts [2] were stably transfected with empty (-/-) or a flag-tagged N-WASP (Flag N-WASP) vectors. Total cellular lysates (10 mg) were then immunoprecipitated with anti-Flag abs. Lysates (lysates) or N-WASP-immunodepleted lysates (ID lysates) (25 μg) (see Fig. 1f) were immunoblotted with the indicated Abs. S1c. Abi1, but not N-WASP, immunoprecipitates with WAVE2. Total cellular lysates of HeLa cells were immunoprecipitated with anti-WAVE2 (WAVE) or an irrelevant ab (ctr), as a control. Lysate (-) or immunodepleted lysates (ID) (25 μg) and IP were immunoblotted (WB) with the indicated Abs. S1d. Gel-filtration profiles of Abi1, N-WASP, WAVE, Sos-1, Eps8 and Abl. Total cellular lysates of growing HeLa cells (3.5 mg) were applied onto a 200-ml prep grade Superose-6-column. An aliquot of each fraction, indicated at the top, was resolved by SDS-PAGE and immunoblotted with the indicated abs. The elution profile of proteins of known molecular weight (M*w*) is indicated at the bottom. The input lane (I) was loaded with 100 μg of total cellular lysates.

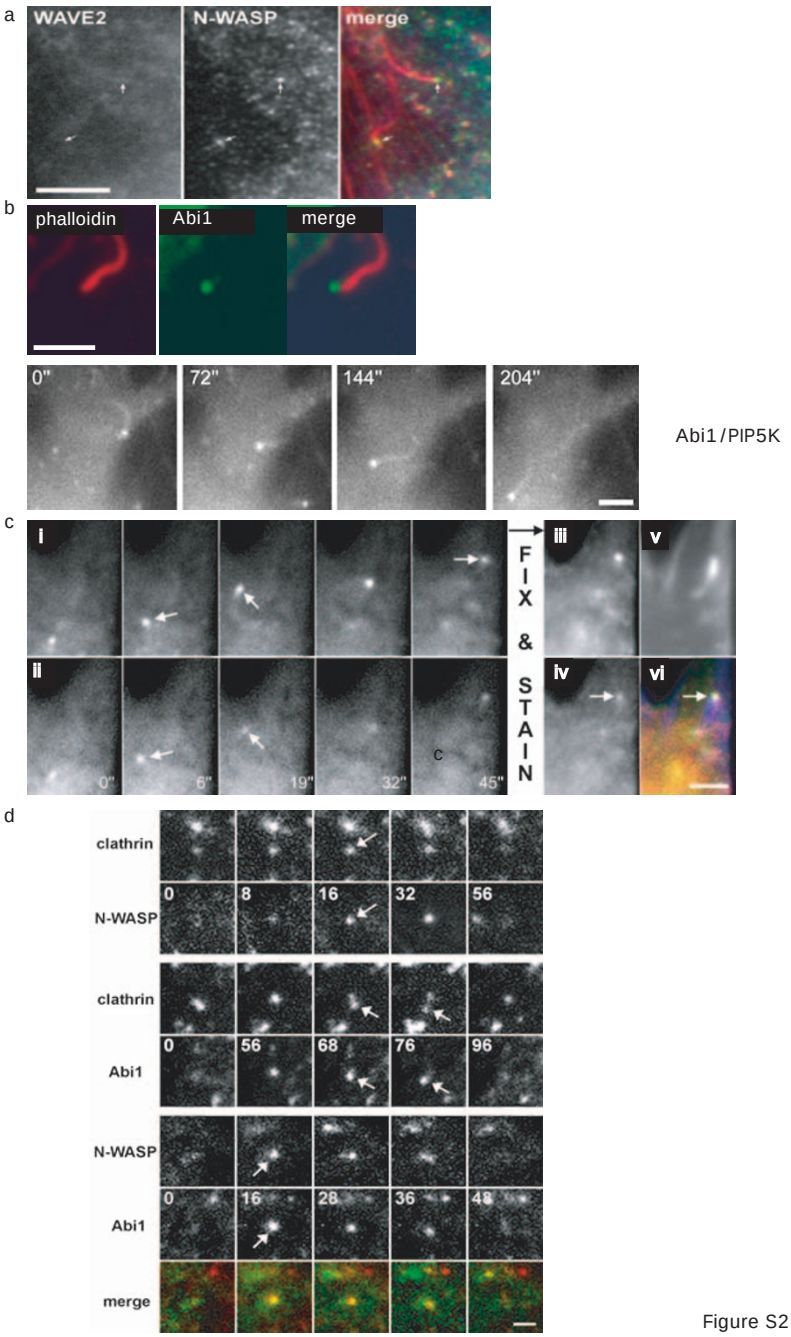

Figure S2. Innocenti et al.

Figure S2a N-WASP and Abi1, but not WAVE2, localize at the surface of PIP5K-induced comets tails. Fibroblast (or HeLa, not shown) cells were co-transfected with GFP-WAVE2 (WAVE2) and myc-tagged PIP5K, fixed and counterstained as indicated for the actin cytoskeleton with phalloidin (red in merge) and for N-WASP (green in merge). Arrows mark the position of N-WASP accumulation at the vesicle-comet interface, which is devoid of WAVE2. Bar equals 5 µm. S2b. Abi1 accumulates on motile vesicles. Fibroblast cells were co-transfected with GFP-Abi1 and myc-tagged PIP5K, and processed for immunofluorescence, as described in Fig. S1a (upper panels), or for time-lapse fluorescence microscopy (lower panels). Selected frames from a video of a cell displaying vesicle rocketing are shown (see also Supplementary Video 3). Note that Abi1 is enriched at the vesicle-comet tail interface, reminiscent of the localization characteristics of N-WASP (Figure 3a and ref. [3]). Time is in seconds and bar equals 3 µm. S2c. Abi1 and N-WASP co-localize on actin-rich motile vesicles. Fibroblast cells were co-transfected with GFP-Abi1, mRFP-N-WASP and PIP5K, and processed for dual-color time-lapse fluorescence microscopy (left panels). Still images representing the dynamics of GFP-Abi1 and mRFP-N-WASP are shown in (i) and (ii), respectively. Cells were then fixed and processed for epifluorescence to detect GFP-Abi1 (iii) or mRFP-N-WASP (iv) after fixation and counterstained with Alexa350-phalloidin (v). Merged image is shown in (vi) (false colors: Abi1 green, N-WASP red, phalloidin blue). Bar is 2 µm. S2d. Ectopically expressed N-WASP and Abi1 can accumulate at internalizing clathrin coated pits. Fibroblast cells co-expressing mRFP-clathrin and GFP-N-WASP (upper panels), mRFP-clathrin and GFP-Abi1 (middle), or mRFP-Abi1 (red in merge) and GFP-N-WASP (green in merge) (bottom panels) were examined by dual-color total internal reflection fluorescence (TIRF) video microscopy. As observed with N-WASP [4,5] [Benesch et al. in press [1]], Abi1 can localize to clathrin coated structures shortly before their internalization. In addition, N-WASP and Abi1 can co-accumulate on internalizing pit-like structures (bottom panels and merge). Arrows denote respective co-localizations. Time is in seconds and bar equals 1 µm.

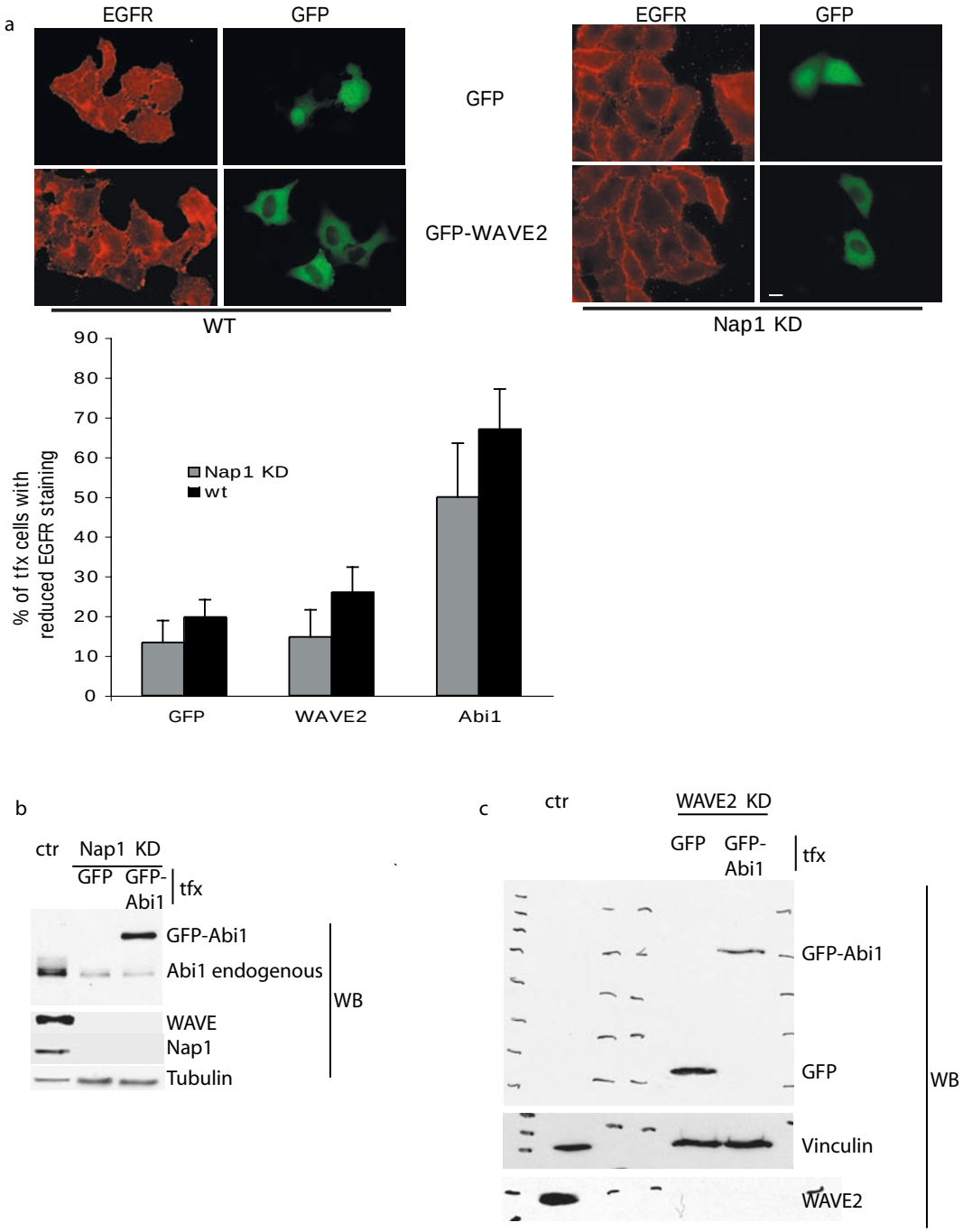

Figure S3a Expression of WAVE2 has no effect on plasma membrane EGFR levels either in wild type or in Nap1 knock down cells. Control (Wt) HeLa and Nap1 KD (Nap1 KD) cells were transfected with GFP-WAVE2 (GFP-WAVE2) or the empty vector (GFP). After serum starvation, cells were fixed. Anti-EGFR ab recognizing an extracellular epitope, was used *prior* to permeabilization to detect cell-surface EGFR. Transfectants were identified using GFP epifluorescence. Bar is 10 μm. *Bottom graph.* The percentage of transfected cells with reduced EGFR staining is indicated in the histogram. The ectopic expression of Abi1 was used as positive control (see also Fig 3a). Data are expressed as the mean ± s.e.m. of three independent experiments where more than 100 cells for each experiment were counted. S3. b. Transient expression of Abi1 is not sufficient to restore the expression of WAVE in Nap1-1 KD cells. Total cellular lysates obtained from control HeLa (ctr), or Nap1 KD cells transfected with GFP or GFP-Abi1 (tfx), as described in Fig. 3C, were immunoblotted (WB) with the indicated abs. No expression of WAVE2 could be detected upon GFP-Abi1 expression in Nap1 KD cells. S3c. Expression levels of GFP or GFP-Abi1 ectopically transfected into WAVE2 KD cells. Total cellular lysates obtained from control HeLa (ctr), or WAVE2 KD cells transfected with GFP or GFP-Abi1 (tfx), as described in Fig. 3C, were immunoblotted (WB) with the indicated abs.

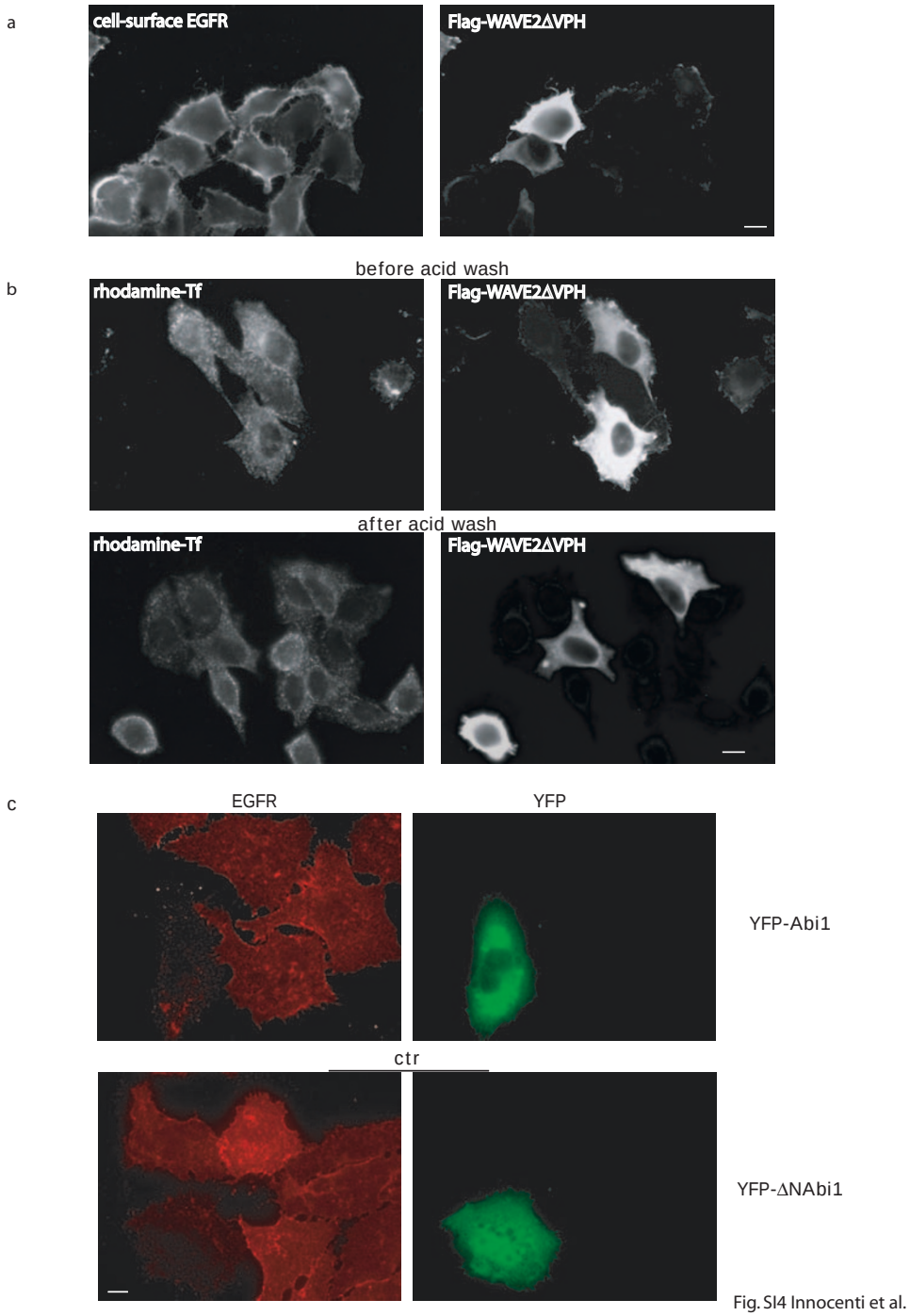

Fig. SI4 Innocenti et al.

Figure S4a A WAVE2 dominant negative does not affect the levels of cell-surface EGFR and TfR. HeLa cellswere transfected with flag-tagged WAVE2ΔVPH (Flag-WAVEΔVPH) construct, which lacks he Verprolin Homology domain of WAVE2 and was shown to act as a dominant negative[7]. Cells were then serum starved for 16 hours and processed to determine the level of cell-surface EGFR (a, top panels) as described in Fig. 4. Alternatively, serum starved transfected cells were incubated in the presence of rhodamine-conjugated transferrin (rhodamine-Tf) and either washed with PBS (before acid wash) or with ice cold 0.2M acetic acid (pH 2.8) containing 0.5M NaCl for 5min (after acid wash), before fixation and staining as described in Fig. 5. Acid wash strips cell surface-receptor-bound transferrin. Bars are 10 μm. S4b. The expression of Abi1 or an Abi1 mutant, which no longer binds to WAVE2, decreases the levels of cell-surface EGFR. HeLa cells transfected with YFP-Abi1 or YFP-ΔN-Abi1, which lacksthe first 145 amino acidsencompassing the binding surface for WAVE [8,9], were serum starved, fixed and processed to determine the level of cell-surface EGFR as described in Fig. 4. Bars are 10 μm. A similar decrease of cell surface EGFR could also be observed in Abi1 KD cells transfected with YFP-DN-Abi1 (not shown).

Movie S1a-b Three-D reconstructions from confocal Z-section series of Abi1- and N-WASP-containing comet tails. HeLa cells were co-transfected with GFP-Abi1 (Abi1) or GFP-N-WASP (N-WASP) and myc-tagged PIP5K, fixed and processed for epifluorescence to visualize GFP-proteins (green), and stained with phalloidin or anti-myc to detect F-actin (red) or PIP5K (not shown), respectively. Still images are shown in Fig. 2a. Confocal sections (60) were taken every 300 nm along the Z-axis, and three-D reconstruction was obtained using ImageJ software.

Movie S2 GFP-Abi1 rocketing by actin-based motility at the surface of PI5K-induced vesicles. Fibroblast cells were co-transfected with GFP-Abi1 and myc-tagged PIP5K, and processed for epifluorescence video microscopy. Display rate is 144x.

Movie S3 Enhancement of the motility of N-WASP-containing pit-like structures by co-overexpression of Abi1. N-WASP null fibroblasts [3] co-overexpressing GFP-N-WASP and mRFP-Abi1 were examined by dual-color time lapse TIRF microscopy. Note the virtually complete co-localisation of the ectopically expressed proteins in structures reminiscent of pit-like accumulations as observed at low expression levels for both proteins (see Figure S3). The enhanced lateral mobility of these pit-like structures, moderate levels of which were reported to frequently precede or accompany the disappearance from the plane of illumination and hence pit internalization [4,5] is indicative of increased N-WASP activity effected by Abi1 overexpression, since this phenotype was not observed in cells with low expression levels of the latter protein as exemplified in Figure S3). Display rate is 40x.

Movie S4 Latrunculin A treatment blocks the motility of N-WASP and Abi-1-containing pit-like structures. N-WASP null fibroblasts [3] co-expressing GFP-N-WASP and mRFP-Abi1 were examined by dual-color time lapse TIRF microscopy. The observed motility of N-WASP and Abi1-containing structures required actin polymerization, since it was abruptly arrested by addition of Latrunculin A (0.5µM) and restored upon washout of the drug as indicated.

SUPPLEMENTARY METHODS.

The mRFP-clathrin construct and the experimental setup employed for dual-colour through the objective TIRF microscopy will be described elsewhere (Benesch et al., in press [1]). mRFP-Abi1 was generated by exchanging EGFP for mRFP (kindly provided by Roger Y. Tsien) in EGFP-Abi1. For video microscopy of cells ectopically expressing PI5K or for examination by TIRF illumination, fibroblasts were routinely grown on glass-coverslips coated with 50µg/ml fibronectin (Roche). Single- or dual-color epifluorescence video microscopy was performed essentially as described (Steffen et al., 2004) employing a 100x, 1.4NA objective with or without 1.6 intermediate optovar magnification.

For counterstaining of the actin cytoskeleton of the PI5K/Abi/N-WASP expressing cell in Figure S2c, the coverslip was fixed on the microscope stage with 4% formaldehyde (20 minutes) and permeabilized with 0.1% Triton X-100 (30 seconds), followed by staining with Alexa Fluor 350 coupled phalloidin (Invitrogen). Images were acquired in PBS containing 100mM dithioerythritol to avoid photobleaching.

Latrunculin A was purchased from SIGMA.

1. Benesch, S. et al. N-WASP deficiency impairs EGF internalization and actin assembly at clathrin coated pits. *J. Cell Sci* **In press**(2005).
2. Lommel, S. et al. Actin pedestal formation by enteropathogenic Escherichia coli and intracellular motility of Shigella flexneri are abolished in N-WASP-defective cells. *EMBO Rep* **2**, 850-7 (2001).
3. Benesch, S. et al. Phosphatidylinositol 4,5-biphosphate (PIP2)-induced vesicle movement depends on N-WASP and involves Nck, WIP, and Grb2. *J Biol Chem* **277**, 37771-6 (2002).
4. Merrifield, C.J. Seeing is believing: imaging actin dynamics at single sites of endocytosis. *Trends Cell Biol* **14**, 352-8 (2004).
5. Merrifield, C.J., Feldman, M.E., Wan, L. & Almers, W. Imaging actin and dynamin recruitment during invagination of single clathrin-coated pits. *Nat Cell Biol* **4**, 691-8 (2002).
6. Innocenti, M. et al. Mechanisms through which Sos-1 coordinates the activation of Ras and Rac. *J Cell Biol* **156**, 125-36. (2002).
7. Suetsugu, S., Miki, H. & Takenawa, T. Identification of two human WAVE/SCAR homologues as general actin regulatory molecules which associate with the Arp2/3 complex. *Biochem Biophys Res Commun* **260**, 296-302 (1999).
8. Stradal, T. et al. The Abl interactor proteins localize to sites of actin polymerization at the tips of lamellipodia and filopodia. *Curr Biol* **11**, 891-5. (2001).
9. Innocenti, M. et al. Abi1 is essential for the formation and activation of a WAVE2 signalling complex. *Nat Cell Biol* **6**, 319-27 (2004).